BULLETIN OF THE POLISH ACADEMY OF SCIENCES
TECHNICAL SCIENCES
Vol. 54, No. 3, 2006

Parameter independent encoderless control of servo drives without additional hardware components

R. KENNEL*, O.C. FERREIRA, and P. SZCZUPAK

Institute for Electrical Machines and Drives, Rainer-Gruenter-Strasse 21, Wuppertal University, D-42119 Wuppertal, Germany

Abstract. A lot of methods for sensorless drive control have been published last years for synchronous and asynchronous machines. One of the approaches uses high frequency carrier injection for position control. The injected high frequency signal is controlled to remain in alignment with the saliency produced by the saturation of the main flux. Due to the fact that it does not use the fundamental machine model which fails at standstill of the magnetic field it is possible to control the drive even at zero speed. In spite of this obvious advantage industry does not apply sensorless control in their products. This is due to the dependency of many published methods on physical parameters of the machine. The high frequency carrier injection method, presented in this paper, does not need to have exact machine parameters and it can be used for machines where there is only a very small rotor anisotropy like in Surface Mounted Permanent Magnet Synchronous Machines (SMPMSM) [1].

Standard drives usually are supplied by a 6-pulse diode rectifier. Due to new European directives concerning the harmonic content in the mains it is expected that the use of controlled pulse-width modulated PWM rectifiers will be enforced in the future [2]. An important advantage of this type of rectifiers is the regeneration of the energy back to the grid. Another benefit are low harmonics in comparison to diode rectifiers. Using one of many control methods published so far it is also possible to achieve almost unity power factor. However, in these methods voltage sensors are necessary to synchronize PWM rectifiers with the mains. Therefore they are not very popular in the industry with respect to the cost and the lack of reliability. Recently a control method was proposed which is based on a tracking scheme. It does not need any voltage sensor on the ac-side of the rectifier and it does not need to know accurate parameters of the system.

This paper presents the control solution for a cheap, industry friendly (no additional hardware and installation effort) drive system. The phase tracking method for control of electrical drive and PWM rectifier is described. Encouraging experimental results are shown.

Key words: sensorless control, high frequency injection, PMSM, active rectifier, PWM rectifier.

1. Introduction

1.1. High frequency signal injection. Many new estimation algorithms for speed detection or even position detection of synchronous machines at low and zero speeds have been proposed. High frequency injection methods are gaining more and more attention [3–5]. Injection methods are normally not applied to Surface Mounted Permanent Magnet Synchronous Machines (SMPMSM), because the magnets are distributed rather homogenously on the surface of the rotor resulting in very small saliencies.

This paper refers to a concept published in [1], which takes advantage of a fact, that these machines in spite of their homogenous design provide a small amount of anisotropy produced by saturation of the main flux. The high-frequency test signal is controlled to be in alignment with the saliency induced by saturation. The injection signal can be described as an amplitude modulated space vector. A synchronous tracking scheme evaluates the anisotropy – this concept avoids complex demodulation algorithms which are sensitive to variations of machine parameters and additional saliencies neglected by the model.

1.2. Active PWM rectifier. Schematically a PWM rectifier setup can be shown as in Fig. 1. There are a lot of different sensorless controll methods for the PWM rectifiers [6–8]. In [9] a simple sensorless control strategy for PWM rectifier was presented with the estimation method of the grid voltage capable to reach unity power factor and insensitivity against parameter variations like inductance saturation interconnecting the grid voltage and output voltage of the converter.

This paper combines the proposals of [1] and [9] resulting in a parameter independent sensorless drive control for synchronous machines with permanent magnets. It shows also behaviour of the proposed method in case of a disconnection of one of the grid phases. The control method is applicable to PWM drive converters without hardware changes whether they use space vector modulation method or hysteresis based modulations.

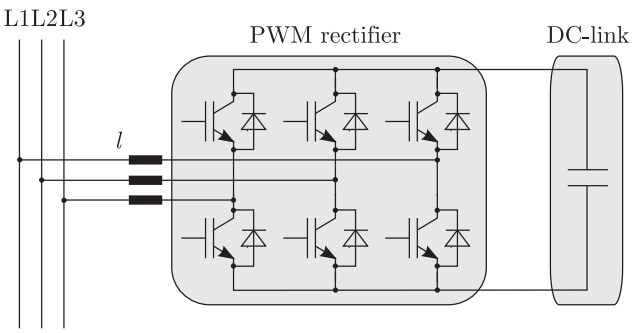

Fig. 1. Scheme of the 3-phase PWM input rectifier system

*e-mail: kennel@ieee.org

2. Alternating carrier injection principle

The phase angle of an alternating carrier voltage vector $\boldsymbol{u}_c$ is kept in alignment with the estimated d-axis in the dq-rotor reference frame (Fig. 2). As a consequence, the modulation has almost no effect on the torque producing current component in the q-axis [10].

Based on this approach the superimposed carrier signal can be described in stator coordinates as follows

$$\boldsymbol{u}_c^{(S)} = u_c \cos(\omega_c t) e^{j\hat{\omega} t}. \tag{1}$$

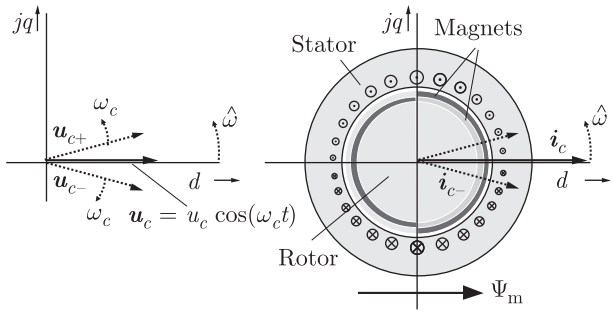

Fig. 2. Resulting current signal i_c as a modulated space vectors in rotor coordinates

The carrier frequency ω_c is chosen around 2 kHz to obtain a fast response and to avoid interaction with the current control loop. As long as the estimated rotor position coincides with the real rotor position δ the test signal is a composition of two high frequency test signals as used in conventional high-frequency injection methods [11] but rotating in directions opposite to each other. As a result only the d-axis is excited by the carrier (see Fig. 2). The resulting high-frequency current $\boldsymbol{i}_c$ (response of the electromagnetic circuits to the injection voltage $\boldsymbol{u}_c$) is also in alignment with the main flux. Like the voltage the current can be also decomposed to a positive and negative sequence component, i_c- and i_c+ respectively (Fig. 2). The amplitude of $\boldsymbol{i}_c$ varies sinusoidally with time. A small misalignment between the real and the estimated rotor position produces an additional high frequency component

$$\boldsymbol{i}_c^{(\hat{\delta})} = \frac{u_c}{l_d l_q} \sin(\omega_c t)[l_d + (l_q - l_d) e^{-j(\hat{\delta}-\delta)}], \tag{2}$$

which can be detected to feed a rotor saliency tracking algorithm which is sensitive even to the small anisotropies of SMPMSMs [10]. The current signal (2) is not used to estimate the rotor position by calculations. It serves as an error signal that is minimized by the tracking scheme in the next sampling cycle.

3. Estimation of the anisotropy

The novel method generates a positive as well as a negative current sequence component(see Fig. 2), both containing information about the rotor position. The injected carrier voltage

$$\boldsymbol{u}_c^{(S)} = u_c \cos(\omega_c t) e^{j\hat{\delta}_a} \tag{3}$$

is always in alignment with the estimated position of the anisotropy (estimated values are marked with a hat$\hat{}$):

$$\hat{\delta}_a = \hat{\omega}_a t. \tag{4}$$

The anisotropy in a SMPMSM is mainly based on the saturation effect of the main flux; it rotates with the same frequency ω as the rotor itself. In difference to the field oriented system the subscript a generally indicates an anisotropy-aligned coordinate system. Both coincide in the case of surface mounted PMSM.

A transformation of the carrier voltage to field coordinates is done by multiplying Eq. (3) by $e^{-j\delta}$. Consequently the differential stator equation can be represented as follows:

$$\boldsymbol{u}_c^{(F)} = u_c \cos(\omega_c t) e^{j(\hat{\delta}-\delta)} = \boldsymbol{l}_\sigma^{(F)} \frac{d\boldsymbol{i}_c^{(F)}}{dt}. \tag{5}$$

Stator resistance, induced voltage and cross coupling of the currents are neglected in the differential stator equation [10]. This is only permitted if the carrier frequency ω_c is much higher than the fundamental frequency (f_i = 2kHz).

The real field angle δ is the unknown variable in this equation. The solution of (5) in field coordinates is

$$\boldsymbol{i}_c^{(F)} = \frac{u_c}{\omega_c} \sin(\omega_c t) \left[\frac{1}{l_{\sigma d}} \cos(\hat{\delta} - \delta) + j \frac{1}{l_{\sigma q}} \sin(\hat{\delta} - \delta) \right]. \tag{6}$$

Equation (6) can be discussed as follows: the carrier current amplitude $|\boldsymbol{i}_c|$ increases proportionally to the carrier voltage $\boldsymbol{u}_c$ and decreases with increasing carrier frequency. Moreover, the carrier current component i_{cq} is directly proportional to the angle error $\Delta\delta$.

This offers an effective way to demodulate the rotor position information. For small angles the $\sin$-function from (6) behaves proportionally to the angle error $\Delta\delta$. Hence, the next processing cycle is used to correct the direction of carrier signal.

4. Sensorless control approach

Using high frequency injection methods for sensorless control, the signal demodulation algorithm requires high performance in signal processing. To reduce the calculation effort, the high-frequency current $\boldsymbol{i}_c$ (6) is transferred to a reference frame in a negative direction at approximate carrier frequency. This is done by

$$\boldsymbol{i}_c^{(\omega_c t + \hat{\delta})} = \boldsymbol{i}_c^{(S)} e^{-j(\omega_c t + \hat{\delta})}, \tag{7}$$

where $\boldsymbol{i}_c^{(S)}$ is the injected current in stator coordinates.

This transformation generates a high frequency current signal that is easy to demodulate without referring to machine parameters. Assuming the remaining negative sequence current components of $\boldsymbol{i}_c$ are rejected by a low pass filter, transformation (7) applied to the current signals (6) results in

$$\boldsymbol{i}_p^{(\omega_c + \hat{\delta})} = u_c \frac{1}{j4\omega_c l_{\sigma d} l_{\sigma q}} \begin{pmatrix} (l_{\sigma d} + l_{\sigma q}) \\ -(l_{\sigma d} + l_{\sigma q}) e^{j(2\delta - 2\hat{\delta})} \end{pmatrix}. \tag{8}$$

It can easily be separated because it is transformed by (7) to about twice the carrier frequency.

Equation (8) illustrates the current response containing the useful information about the misalignment of the estimated field angle with reference to the real field angle. It is used as an error estimation angle

$$\Delta\delta = \delta - \hat{\delta}. \tag{9}$$

The current response is further simplified to reduce processing power necessary for demodulation. In the case of small error estimation angles the current response is:

$$\boldsymbol{i}_p^{(\omega_c+\hat{\delta})} = u_c \frac{1}{4\omega_c l_{\sigma d} l_{\sigma q}} \begin{pmatrix} -j(l_{\sigma d}+l_{\sigma q}) \\ -(l_{\sigma d}+l_{\sigma q})2\Delta\delta \end{pmatrix}. \tag{10}$$

This equation shows the real component of the current response in the reference frame according to (7) being proportional to the error angle $\Delta\delta$. This is used to track the field angle by a closed loop tracking system (Fig. 3).

As discussed in [1] the signal flow graph in Fig. 3 illustrates the basic structure of the proposed sensorless scheme. The current signal is sampled with the sampling frequency of the current control loop. The following PI-controller feeds a controlled oscillator to create the estimated field angle. This results in a closed loop structure that corrects the field angle stepwise by each sampling cycle. Hence, a high sampling frequency ensures good and dynamical fast alignment with field axis. The disturbances of the acquired signal are low, thus permitting operation at low carrier amplitudes. The prominent advantage is the tracking observer not depending on any machine parameters.

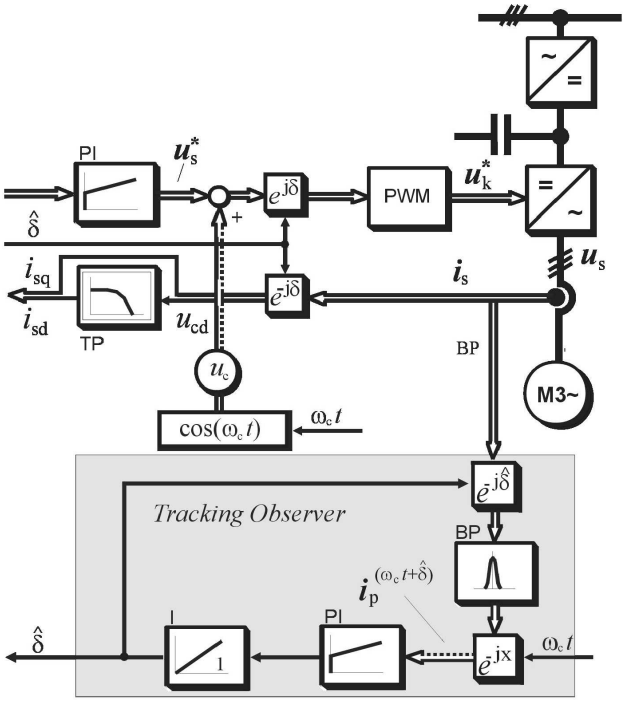

Fig. 3. Signal flow graph of the field angle estimation scheme based on the proposed method

5. Voltage oriented control for PWM rectifier

Space vector notation of PWM rectifier electrical circuit supports a clear understanding of the physical quantities of components and their behavior [12].

Figure 4 shows a model of the PWM rectifier system used for the analysis. The line current vector $\boldsymbol{i_s}$ is controlled by the converter and is directly related to the voltage drop across the inductance $\hat{l}_s$. The inductance is necessary to reduce the high harmonic switching content in the current caused by the switching of the rectifier and to decouple the supply voltage from the converter output voltage. The inductance voltage $\hat{\boldsymbol{u}}_{\boldsymbol{ls}}$ is equal to the difference between the grid voltage $\hat{\boldsymbol{u}}_{\boldsymbol{grid}}$ and the converter voltage $\boldsymbol{u}_{\boldsymbol{conv}}$.

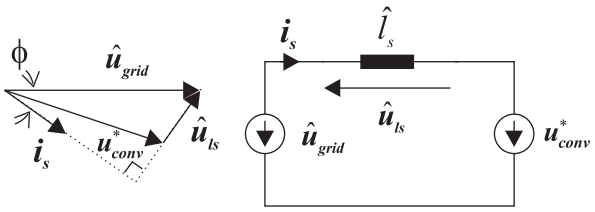

Fig. 4. Model of the PWM rectifier system

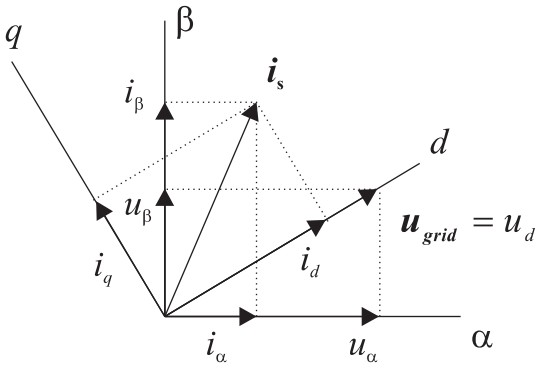

Fig. 5. Coordinate transformation from fixed $\alpha\beta$ to rotating *dq* reference frame

Using conventional voltage oriented control all quantities are referred to a synchronous reference frame aligned with the supply voltage. Therefore the control scheme is based on coordinate transformation between stationary $\alpha\beta$- and synchronous *dq*-reference system (Fig. 5).

In the *dq* reference frame, the AC-line current vector $\boldsymbol{i_s}$ is divided into rectangular components. The component i_q determines the reactive power whereas i_d determines the active power flow. If i_q is controlled to zero the minimum current for a given reactive power is ensured and the power factor is one.

As in steady state the stator voltage can normally be considered sinusoidal, the voltage and flux orientation becomes equivalent except to ninetydegrees phase shift. This encouraged to consider the grid as a machine and apply the well-known principle of field orientation. This leads to the same simple and reliable principle as in revolving field machines. The equations for the PWM rectifier system in the *dq* reference frame are:

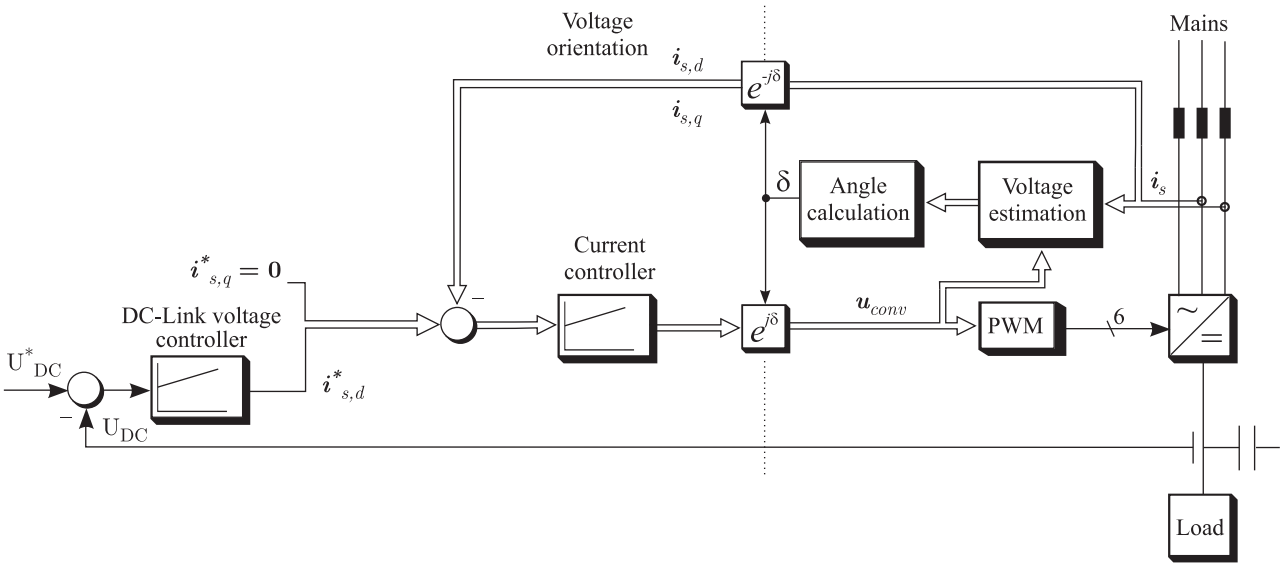

Fig. 6. Sensorless Voltage Oriented Control

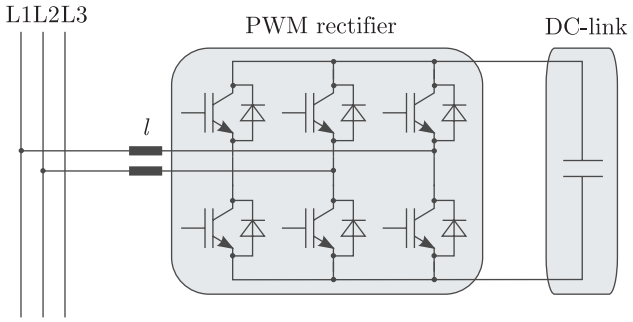

Fig. 7. Single grid phase ($L3$) disconnection

$$\hat{u}_d = l\frac{di_d}{dt} + u_{d,conv} - \omega_s l i_q \qquad (11)$$
$$0 = l\frac{di_q}{dt} + u_{q,conv} + \omega_s l i_d.$$

Usually the line voltages must be measured for calculation of the voltage angle necessary for coordinate transformation. To reduce costs of the system, there is a possibility to estimate the line voltage. The estimated voltage is used to calculate a voltage angle. Coordinate transformation from fixed $\alpha\beta$ coordinates to rotating *dq* reference frame is done using the estimated voltage angle.

6. Sensorless voltage oriented control

Based on the PWM rectifier system model, the grid voltage estimation is proposed to be a phase tracking method. The current $\boldsymbol{i_s}$ passing inductance $\hat{l}_s$ is causing a voltage $\boldsymbol{\hat{u}_{ls}}$. This voltage can be calculated as:

$$\hat{u}_{l,\alpha} = l\frac{di_\alpha}{dt} \qquad (12)$$
$$\hat{u}_{l,\beta} = l\frac{di_\beta}{dt}$$

while estimated grid voltage $\boldsymbol{\hat{u}_{grid}}$ is represented by equations:

$$\hat{u}_{grid,\alpha} = \hat{u}_{l,\alpha} + u_{conv,\alpha} \qquad (13)$$
$$\hat{u}_{grid,\beta} = \hat{u}_{l,\beta} + u_{conv,\beta}.$$

As the currents depend on the voltage difference, any current variation results in voltages over the inductance; this voltage is considered when calculating the next sample period. This scheme tracks continuously the real voltage vector. Figure 6 shows the proposed sensorless control scheme.

When the inductance value is estimated lower than the real inductance value, the system will still find and detect the voltage vector, but the dynamic response will decrease. This can be explained by the dynamic transfer function of the tracking method. Equation (14) shows, that the dynamic response of the phase tracking estimation method decreases with increasing factor k, while k is the relation between the real and estimated inductance $l_s/\hat{l}_s$.

$$\hat{u}_{grid} = \frac{u_{grid}}{T_s k + 1}. \qquad (14)$$

For the smallest possible factor $k = 1$ the fastest step response can be expected. Faster responses $(k < 1)$ lead to instability of the estimation scheme.

7. Phase disconnection problem

For proper operation of the 3-phase PWM rectifier controlled by sensorless Voltage Oriented Control the availability of all the grid phases is essential. If there is a phase disconnection (as shown in Fig. 7) the system cannot work any more due to the lack of the rotating coordinate system. The transformation from stationary $\alpha\beta$- to the rotating dq-coordinate system is not possible any more. The DC-link voltage and the supply current cannot be controlled which my cause a destruction of the rectifier or at least an interruption of the drive system operation.

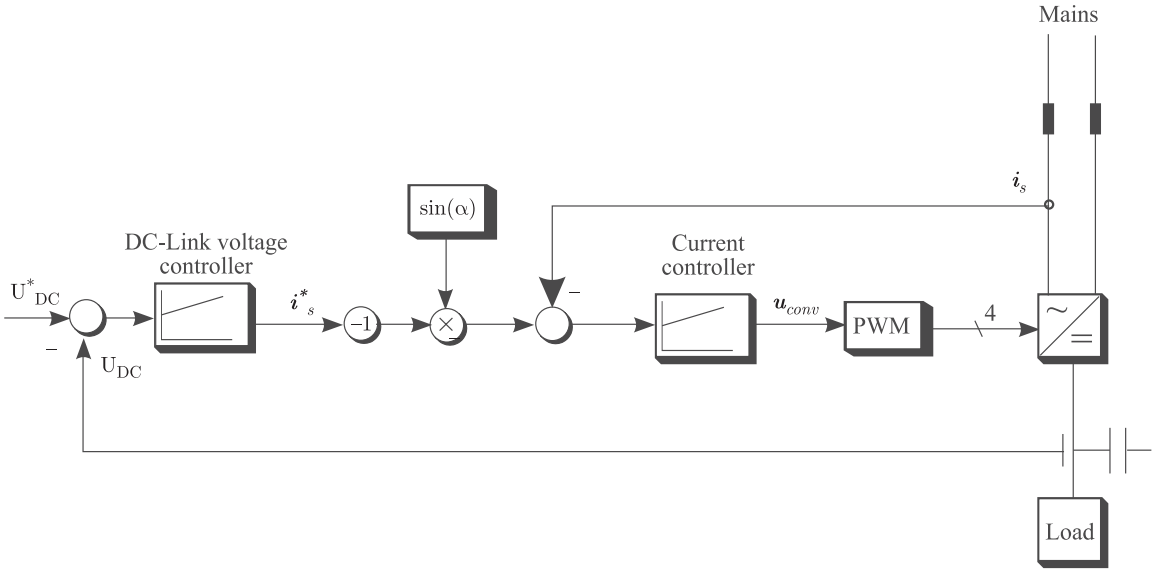

Fig. 8. Control of the PWM rectifier in case of phase disconnection

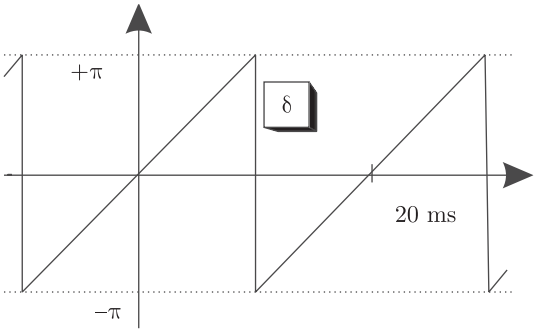

Fig. 9. Voltage angle δ

For the conformity with the industry needs, the PWM rectifier should be able to withstand such a disconnection during a time of at least 5 cycles of the grid voltage (100ms for the 50Hz voltage supply system). The DC-link voltage should be kept constant and the supply current should be in phase with the grid voltage and sinusoidal in spite of the phase disruption. In order to achieve this goal the sensorless "phase tracking" control method has to be modified.

In case of grid phase disconnection the control structure can be explained using Fig. 8. It looks similar to the structure presented in Fig. 6. From the superposed control loop, DC-link voltage control, the magnitude of the reference current is achieved. This is then multiplied with the $\sin(\alpha)$ signal to get the reference current. After comparison with the measured $\boldsymbol{i_s}$ there is a fast current control loop with PI controller with a voltage reference forwarded to the PWM modulator. As one grid phase is disconnected the according leg of the PWM rectifier cannot be used. Therefore only 4 PWM signals are sent to the IGBTs.

The phase shift and frequency of the real current $\boldsymbol{i_s}$ is controlled with an estimated $\sin(\alpha)$ signal generated based on the information from the period, before the phase disconnection occurred. From the estimated $\hat{u}_{l,\alpha}$ and $\hat{u}_{l,\beta}$ voltages the voltage angle δ is calculated using the $\arctan$ function.

During the normal operation (where all three phases are present) the frequency f of the grid voltage is calculated. The angle δ changes from $+\pi$ to $-\pi$ every 20ms (in case of 50Hz). It is very easy to detect this step in the angle and to calculate the voltage frequency from it.

$$f = kf_{sampling} \tag{15}$$

where k is equal to the number of samples taken between the angle steps.

Knowing the frequency it is necessary to find out which phase is disconnected to calculate proper phase shift of the current. Suppose there is no $L3$ in the system. The only voltage which is left is U_{L1-L2}. Current i_s should be now in phase with this voltage.

Knowing that, it is possible to calculate proper phase shift (ϕ) using the last estimated value of the $\hat{\boldsymbol{u}}_{\boldsymbol{grid}}$. From the knowledge of the phase shift and the frequency signal $\sin(\alpha)$ is achieved, where $\alpha = \omega t + \phi$ and $\omega = 2\pi f$.

Of course the scheme has some disadvantages. First: the amplitude of the grid voltage has to be calculated in order to get $\sin(\alpha)$ signal. It is also supposed, that it does not changes during the voltage disconnection. Second: all three grid voltages (U_{L1-L2}, U_{L2-L3} and U_{L3-L1}) have to be estimated during the conventional 3-phase operation of the PWM rectifier.

8. Test results

The experimental results are obtained using a commercial 6-pole SMPMSM servo drive:

Table 1
SMPMSM parameters

Rated power	1.2 kW
Rated speed	6000 rpm
Rated voltage	400 V
Rated current / max. current	2.8/15.2 A

The rectifier parameters used in the laboratory set-up are:

Table 2
Laboratory set-up parameters

Nominal line voltage	230 V_{rms}
Nominal line current	7 A_{rms}
Grid filter inductance l_s	3.5 mH
Grid filter resistance r_s	50 mΩ
DC-Link capacitor C	750 µF
Nominal DC-Link voltage U_{DC}	750 V
Switching frequency f	4 kHz

8.1. Sensorless PMSM control. The estimated position $\hat{\delta}$ is used as a feedback signal for field oriented control. The central track of the diagram in 10 represents the position error $\Delta\hat{\delta}$ between the measured position δ and the estimated position $\hat{\delta}$. The switching frequency is 8 kHz, the carrier frequency is 2 kHz with a peak carrier current i_c, max of 200 mA. The current control is processed using the same 12-Bit A/D converter also used for sensing the fundamental currents.

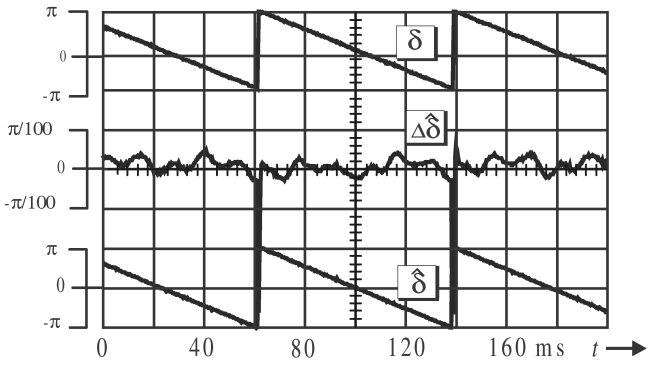

Fig. 10. Experimental results: rotor position δ and corresponding estimated variables $\hat{\delta}$

8.2. Sensorless PWM rectifier

Nominal PWM rectifier operation. PMW rectifier was supplied from a standard 400V, 50Hz grid. Figure 11 shows the supply voltage u_α and line current i_α, which are in phase It means, that the rectifier works properly and the power factor is high. The line current is sinusoidal although there is a harmonic content in the grid voltage.

Grid phase disconnection. Tis paper shows also the behaviour of the modified "phase tracking" control scheme when there is a grid phase disconnection. The disconnection was made in phase $L3$. It is important to notice, that the $L3$ phase current is not measured by a current sensor. It is calculated from the measured $L1$ and $L2$ currents. Nevertheless the proposed method works fine.

Figure 12 shows the PWM rectifier keeping the DC-link voltage constant during more then 5 cycles of the grid voltage during phase disconnection. The phase current of the other phases remained sinusoidal and had of course to be increased to keep the DC-link voltage at the same level. The pulsation of the DC-link voltage could be minimized by setting the voltage PI controller slower.

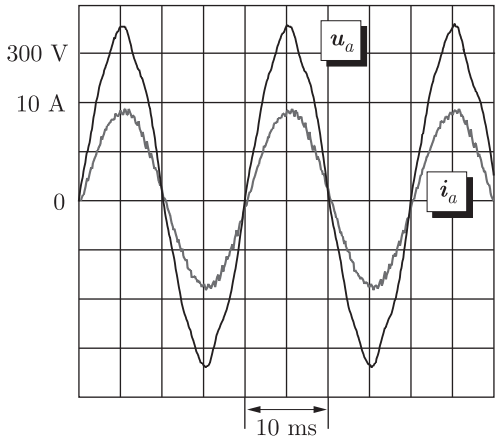

Fig. 11. Line current (α) and supply voltage (α)

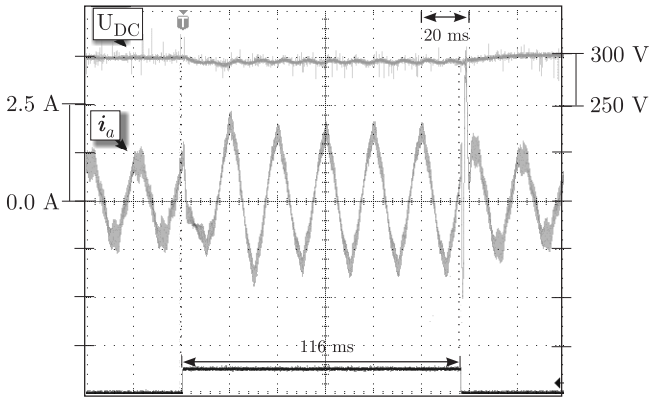

Fig. 12. $L3$ phase disconnection for 116ms. U_{DC} – DC-link voltage, i_a – phase current

9. Conclusions

This paper presents an improved sensorless control algorithm for Surface Mounted Permanent Magnet Synchronous Machines using high-frequency voltage injection. The method is suitable for reluctance machines and permanent magnet machines with buried magnets, but it is especially designed to track small saliencies and to detect the small differences in rotor anisotropy provided by synchronous motors with surface mounted permanent magnets. The position estimation method is independent of machine parameters because the position error is estimated by a tracking scheme.

The sensorless control method based on the Voltage Oriented Control for active PWM rectifiers is also presented. The experimental tests show the advantages of the proposed phase tracking method.It is shown that with a change in control algorithm it is possible to achieve an operation of the rectifier also during phase disconnection.

REFERENCES

[1] M. Linke, R. Kennel, and J. Holtz, "Sensorless speed and position control of synchronous machines using alternating carrier injection", *IEEE Int. Electrical Machines and Drives Conf. IEMDC* 2, 1211–1217 (2003).

[2] J.R. Rodríguez, J.W. Dixon, J.R. Espinoza, J. Pontt, and P. Lezana, "PWM regenerative rectifiers: state of the art", *IEEE Trans. on Ind. Electron.* 52 (1), (2005).

[3] J. Holtz, "Sensorless position control of induction motors - an emerging technology", *IEEE Trans. on Ind. Electron.* 45 (6), (1998).

[4] J.K. Ha and S.K. Sul, "Sensorless field-frientation control of an induction machine by high-frequency signal injection", *IEEE Trans. on Ind. Appl.* 35 (1), (1999).

[5] A.Consoli, F. Russo, and A. Testa, "Low- and zero-speed sensorless control of synchronous reluctance motors", *IEEE Trans. on Ind. Appl.* 35 (5), 1050–1051 (1999).

[6] T.Noguchi, H. Tomiki, S. Kondo, and I. Takahashi, "Direct power control of PWM converter without power-source voltage sensors", *IEEE Trans. on Ind. Appl.* 34 (3), (1998).

[7] T. Ohnuki, O. Miyashita, P. Lataire, and G. Maggetto, "Control of a three- phase PWM rectifier using estimated AC-side and DC-side voltages", *IEEE Trans. on Power Elect.* 14 (2), (1999).

[8] S. Hansen, M. Malinowski, F. Blaabjerg, and M.P. Kaźmierowski, "Sensorless control strategies for PWM rectifier", *APEC 2000* 1, 832–838 (2000).

[9] R. Kennel, M. Linke, and P. Szczupak, "Sensorless control of 4-quadrant- rectifiers for voltage source inverters (VSI)", *Power Electronics Specialists Conference – PESC* 3, 1057–1062 (2003).

[10] M. Linke, R. Kennel, and J. Holtz, "Sensorless position control of permanent magnet synchronous machines without limitation at zero speed", *28th Annual Conf. IEEE Industrial Electronics Society IECON* 1, 674–679 (2002).

[11] R.D. Lorenz, "Sensorless drive control methods for stable, high performance, zero speed operation", *Int. Conf. on Power Electronics and Motion Control- EPE-PEMC* 1, 1–11(2000).

[12] J. Holtz, "The dynamic representation of AC drive systems by complex signal flow graphs", *Conf. Record of ISIE*, Santiago, Chile, 1–6 (1994).